Infrared Physics & Technology 53 (2010) 89–93

Contents lists available at ScienceDirect

Infrared Physics & Technology

journal homepage: www.elsevier.com/locate/infrared

Evaporation of uniform antireflection coatings on hemispherical lenses to enhance infrared antenna gain

Brian A. Slovick *, Peter M. Krenz, Guy Zummo, Glenn D. Boreman

University of Central Florida, College of Optics and Photonics (CREOL), 4000 Central Florida Blvd., Orlando, FL 32816, United States

ARTICLE INFO

Article history:
Received 3 September 2009
Available online 9 October 2009

Keywords:
Infrared antennas
Immersion lens
Antenna-coupled detectors
Antireflection coatings

ABSTRACT

Infrared dipole-coupled bolometers receive radiation more efficiently when illuminated through a high permittivity, antireflection (AR) coated, hemispherical immersion lens. To maintain the enhanced responsivity for all illumination angles, the AR coating must be uniform over the hemispherical surface. An evaporation method for depositing a uniform AR coating on the hemispherical surface is presented. The lens is tilted relative to the source, which can be either electron-beam or thermal, and rotated throughout the deposition. Evaporation at an angle of 70° yields a uniform film with less than 10% thickness variation over a 120° full angle of the hemispherical surface. A theoretical model is developed and compared to profilometer measurements. In all cases, there is general agreement between theory and measurement. A single dipole is fabricated onto the flat surface of an AR-coated germanium immersion lens and the responsivity is measured for both substrate-side and air-side illumination. With a zinc sulfide (ZnS) single-layer AR coating, substrate-side illumination yields a broadside antenna response 49 ± 2.7 times greater than air-side illumination.

1. Introduction

The deposition of antireflection coatings on hemispherical lenses is of considerable interest. Infrared dipole-coupled bolometers exhibit significant signal gain when illuminated through a high permittivity, AR coated hemispherical immersion lens [1–4]. In this context, the gain Γ, or irradiance responsivity ratio, is defined as the ratio between the antenna response when illuminated through the substrate to the response when illuminated from the air-side, and is given by the expression

$$\Gamma = \left(\frac{\varepsilon_{r,\mathrm{lens}}}{\varepsilon_{r,\mathrm{air}}}\right)^{3/2}, \tag{1}$$

where $\varepsilon_{r,\mathrm{lens}}$ and $\varepsilon_{r,\mathrm{air}}$ are the relative permittivities of the lens and air [1,2]. Here, the immersion lens is assumed to be perfectly AR coated. When the curved surface of the immersion lens is not AR coated, the gain decreases dramatically. For example, a germanium lens with a permittivity of $\varepsilon_{r,\mathrm{Ge}} = 16$ in the 10 μm infrared region will generate a broadside signal gain of $\varepsilon_{r,\mathrm{Ge}}^{3/2} = 64$ for a perfectly AR coated lens or a gain of $\varepsilon_{r,\mathrm{Ge}}^{1/2} = 4$ for an uncoated lens [3]. In order to maintain the large signal gain for all illumination angles, the AR coat must be uniform over the hemispherical surface. To ensure impedance matching at the germanium–air interface, the AR coating material must have a refractive index of $n = \sqrt{n_{\mathrm{Ge}} n_{\mathrm{air}}} = 2$. We used zinc sulfide, a low-loss insulator with a refractive index of $n = 2.21$ in the 10.6 μm infrared region. The AR coating is a single-layer of zinc sulfide with a quarter-wave thickness of 1.2 μm.

In telecommunication systems, AR coated spherical lenses may be used as low-cost fiber-to-fiber couplers [5]. Similarly, AR coated hemispherical microlenses can be fabricated onto optical fibers to provide efficient coupling to semiconductor lasers [6]. For these applications, the most common deposition method is low pressure chemical vapor deposition (LPCVD) [7,8]. In this process, the nonplanar substrate is placed in a chamber and heated to around 500° C. Precursor gases are released into the chamber at a relatively high pressure of 0.1–5 torr. The heat induces a reaction and subsequent decomposition of the vapor onto all exposed surfaces of the substrate, regardless of their orientation.

In cases where the CVD recipe is unknown or when the toxicity of the precursors requires an elaborate or expensive experimental set-up, electron-beam or thermal evaporation may be the preferred method. For example, the CVD process for zinc sulfide typically involves separate sources of zinc and sulfur, which can react prematurely to produce highly toxic precursors, including $Zn(C_2H_5)_2$ and H_2S [9]. In addition, the high temperatures involved in a LPCVD process may be incompatible with materials having a low melting point, such as aluminum.

Unfortunately, physical vapor deposition is inherently directional and will produce non-uniform films on curved substrates. In the proposed method, the hemispherical lens is tilted relative

* Corresponding author. Tel.: +1 407 823 2979; fax: +1 407 823 6880.
E-mail address: bslovick@creol.ucf.edu (B.A. Slovick).

1350-4495/$ - see front matter © 2009 Elsevier B.V. All rights reserved.
doi:10.1016/j.infrared.2009.10.001

to the source, and rotated throughout the deposition. Rotation at an angle of 70° generates a relatively uniform film with less than 10% thickness variation over the hemispherical surface. A theoretical model is developed and compared to profilometer measurements.

To test the impact of the ZnS AR coat on the antenna gain, a single dipole is fabricated onto the flat surface of a germanium immersion lens. The irradiance response is measured for both air-side and substrate-side illumination. Substrate-side illumination yields an antenna response 49 ± 2.7 times greater than air-side illumination.

2. Theoretical model

A photograph of the rotating device is shown in Fig. 1. The thermal source is aligned with the center of curvature of the hemispherical lens. The white arrow indicates the rotation direction of the shaft. For this configuration, the film thickness distribution over the hemispherical surface can be derived from a radiometric analysis.

Consider a lens of radius R with its center of curvature coincident with the origin of a Cartesian coordinate system, as shown in Fig. 2a. The evaporation source S, which can be either electron-beam or thermal, is regarded as a point source located on the z-axis a distance d from the center of curvature of the lens. The number of particles per unit time ϕ originating at the source, falling on the infinitesimal surface element dA is given by the product of the intensity I, in particles per steradian per unit time, and the solid angle as

$$\phi = I\Omega = I\frac{dA\cos\psi}{r^2}, \tag{2}$$

where ψ is the angle between the radius vector r and a vector normal to dA. The irradiance E, in particles per unit area per unit time, is given by

$$E = \frac{\phi}{dA} = I\frac{\cos\psi}{r^2} = I\left[\frac{d^2\cos^2\theta - 2dR\cos\theta + R^2}{(d^2 - 2dR\cos\theta + R^2)^3}\right]^{1/2}. \tag{3}$$

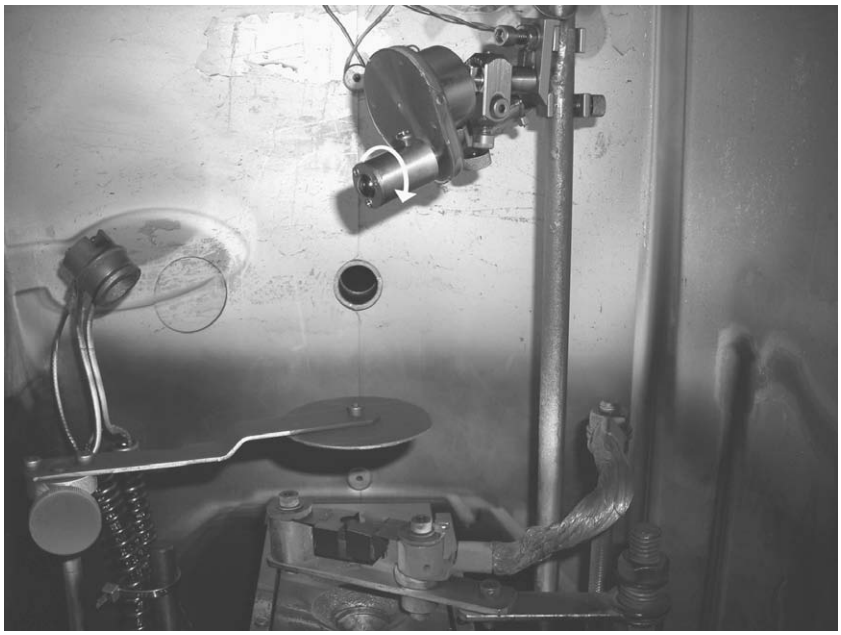

Fig. 1. Photograph of the rotating device inside evaporation chamber. The hemispherical lens is located 14 cm directly above the thermal boat and rotated in the direction indicated by the white arrow.

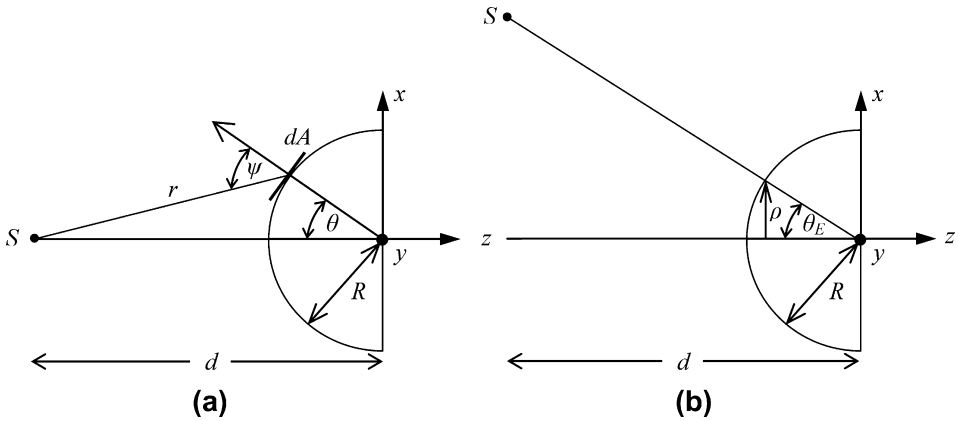

Fig. 2. Definition of terms for the radiometric derivation with a point source (a) on-axis and (b) oriented at an angle θ_E relative to the center of curvature of the lens.

Here the cosine and sine laws were used to eliminate the variables r and ψ and obtain the irradiance in terms of measurable quantities.

If the distance from the source to the center of curvature is much greater than the radius of the lens ($d \gg R$), Eq. (3) simplifies to

$$E \approx E_0 \cos\theta, \tag{4}$$

where $E_0 = I/d^2$ is a constant proportional to the film thickness. Eq. (4) corresponds to the case in Fig. 2a, where the source is aligned with the pole of the hemispherical surface.

In the limit where $d \gg R$, the film thickness distribution can be projected onto the $z = -R$ plane at the front surface of the lens. The coordinates in this plane are related to the angle θ by

$$\sin\theta = \frac{1}{R}\sqrt{x^2+y^2}. \tag{5}$$

Inserting this expression into Eq. (4) and simplifying yields

$$E(x,y) = E_0 \cos\left[\sin^{-1}\left(\frac{1}{R}\sqrt{x^2+y^2}\right)\right] = E_0\sqrt{1-\frac{x^2+y^2}{R^2}}. \tag{6}$$

A change in the evaporation angle shifts the center of the cosine distribution in Eqs. (4) and (6), as shown in Fig. 2b, while the effect of the lens rotation is to average $E(x,y)$ over one angular period. Therefore, the thickness distribution of the rotated hemispherical lens is given by

$$E(x,y;\rho) = \frac{E_0}{2\pi}\int_0^{2\pi}\sqrt{1-\frac{(x-\rho\cos\theta)^2+(y-\rho\sin\theta)^2}{R^2}}d\theta. \tag{7}$$

Here, the notation $E(x,y;\rho)$ denotes the film thickness as a function of the x and y coordinates, evaluated at the spatial offset ρ, which is the x-direction distance from the z-axis to the new center of the cosine distribution, as shown in Fig. 2b. The spatial offset is related to the evaporation angle θ_E by the expression

$$\sin\theta_E = \frac{\rho}{R}, \tag{8}$$

where θ_E is defined in Fig. 2b as the angle between the source and z-axis, measured from the center of curvature. The thickness distribution can be rewritten in terms of the evaporation angle as

$$E(x,y;\theta_E) = \frac{E_0}{2\pi}\int_0^{2\pi}\sqrt{1-\frac{(x-R\sin\theta_E\cos\theta)^2+(y-R\sin\theta_E\sin\theta)^2}{R^2}}d\theta. \tag{9}$$

The integral in Eq. (9) cannot be solved analytically. As a check, Eq. (9) simplifies to the static, non-rotating case of Eq. (6) when the evaporation angle is zero.

3. Method

As shown in Fig. 1, the hemispherical lens is located well above the thermal boat (d = 14 cm, R = 0.5 cm). A crystal thickness monitor is located on the left side of the chamber. The rotating device consists of an electric AC gear motor and a Variac control, which is connected to the gear motor via an electrical vacuum feedthrough. Prior to installation, the motor was out-gassed in a test chamber at ~1 m torr for 36 h. A custom aluminum holder secures the hemispherical lens to the rotating shaft. For all depositions, the rotation rate was set to 0.1 rev. s^{-1} on the external Variac control. The model and results are not dependent on the rotation rate as long as the duration of the deposition is much greater than one rotational period.

Assuming that adhesion and mechanical stress issues are negligible, the model and results are independent of the lens material and evaporant. The hemispherical lens is a high resistivity 3.3 Ω cm germanium lens with a permittivity $\varepsilon_r = 16$, a 10 ± 0.01 mm diameter, a thickness of 5 ± 0.05 mm, and a surface quality of 60/40 scratch/dig. In all depositions, the evaporant is zinc sulfide, a low-loss insulator with a large refractive index of n = 2.21 in the 10 μm infrared region. A BOC Edwards Auto 306 evaporation system, compatible with both electron-beam and thermal sources, is used to thermally evaporate zinc sulfide at a rate of ~1.2 nm s^{-1}. Five film thickness measurements were taken in 15° increments from 0° to 60° using a Veeco Dektak 3 Surface Profiler and variable angle stage. The profilometer scan range was a 300 μm region at the top surface of the lens.

To test the impact of the AR coat on the irradiance responsivity ratio, a single dipole and bolometer were fabricated onto the flat surface of the hemispherical lens using a Leica EBPG5000 + electron-beam writer [10]. A resist bilayer was used, consisting of polymethyl methacrylate–methyl acrylic acid 9% and 150 nm of 950 K polymethyl methacrylate. Both layers were baked on a hot plate at 180 °C for 10 min. Following the exposure, the resist was developed for 60 s in a 1:3 mixture of methyl isobutyl ketone:isopropanol. The fabrication process consisted of two electron-beam writes: one for the antenna, lead lines, and alignment marks, and another to align the bolometer with the feed point of the dipole. For both exposures, the dose and beam current were 620 μC/cm^2 and 25 nA, respectively. The gold antenna and nickel bolometer were deposited using electron-beam evaporation in the BOC Edwards system.

The antenna was illuminated with a CO_2 laser operating at 10.6 μm. The laser was modulated at 2.5 kHz using a mechanical chopper and a bias voltage of 100 mV DC was applied across the antenna [3]. The output signal from the device was measured using a lock in amplifier and a computer with LABVIEW.

4. Results

Fig. 3 contains a cross-sectional plot of Eq. (9) at y = 0 for three different evaporation angles. The thickness is plotted as a function of the incident angle θ defined in Fig. 2a. Since the source distance and intensity remain constant, the theoretical curves can be normalized so that $E_0 = I/d^2 = 1$. In practice, two evaporations are required at each angle: one to determine the thickness for an arbitrary tooling factor, and another with the adjusted tooling factor. The data points are normalized to the theoretical curves using a least squares fit, and the error bars represent one standard deviation above and below the mean.

In agreement with Eq. (4), a cosine distribution is obtained when the evaporation angle is zero. As the evaporation angle is increased to 45°, the thickness at broadside (0°) decreases relative to the thickness at large angles. For an evaporation angle of 70°, the measured thickness variation is less than 10% over a 120° full angle of the hemispherical surface. For larger evaporation angles, the broadside thickness tends to zero. The sharp decrease in thickness that is expected around 20° is not present in the measurements. This feature is an artifact of the model, which assumes that areas not directly exposed to the source receive zero flux. In reality, a moderate amount of residual vapor is expected, and will diminish this feature substantially. To account for this, a constant thickness offset must be added to Eq. (9). This is further justified by the fact that zinc sulfide has a relatively high vapor pressure of ~10^{-5} torr, and may outgas during chamber evacuation.

The thickness offset can be determined from the impingement flux of an ideal gas [11]. By calculating the total number of ZnS molecules impinging on the hemispherical surface over the duration of a deposition, the thickness of a shell of molecules on the lens surface can be determined. During a typical ZnS deposition, the temperature and pressure within the chamber are around

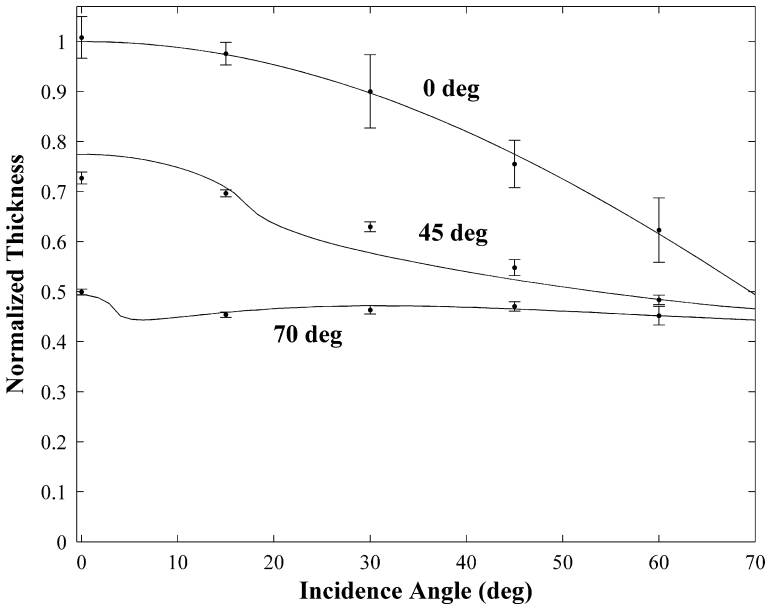

Fig. 3. Film thickness as a function of the incident angle for different evaporation angles. The measurements are normalized to the theoretical curves using a least squares fit, and the error bars represent one standard deviation above and below the mean.

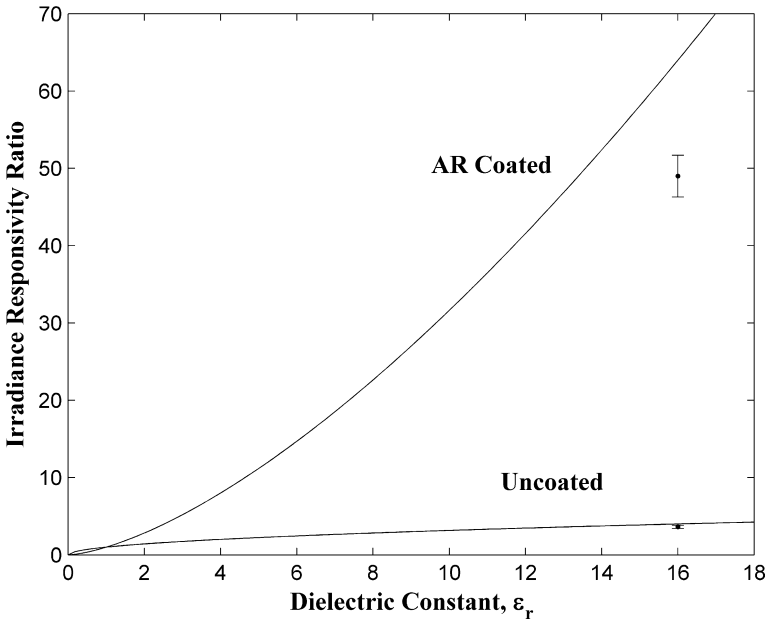

Fig. 4. Irradiance responsivity ratio as a function of the dielectric constant of an uncoated and AR coated immersion lens [3]. The measurements are for a single dipole fabricated onto the flat surface of a germanium immersion lens. The AR coating is a single-layer of zinc sulfide with a quarter-wave thickness of 1.2 μm.

50 °C and 10^{-5} torr, respectively. Under the assumption that the residual vapor behaves as an ideal gas under these conditions, the thickness of a homogeneous shell of ZnS molecules formed on the hemispherical surface during a 15 min deposition is 350 nm, or approximately 30% of the total AR coat thickness of 1.2 μm. Therefore, a thickness offset of $0.3E_0$ is added to Eq. (9) prior to normalization. This has the effect of flattening the distribution over the lens surface.

Unfortunately, the reflectance at the curved surface cannot be measured directly, since reflections from the flat surface are also present. However, a gain measurement can provide information regarding the performance of the AR coating. In Fig. 4, the theoretical broadside gain is plotted for both an uncoated and AR coated lens [3]. For the uncoated germanium lens with permittivity $\varepsilon_{r,\mathrm{Ge}} = 16$, the measured gain was 3.6 ± 0.2 in good agreement with the theoretical value of 4. The measured gain for the AR coated lens was 49 ± 2.7, a significant increase, but less than the expected value of 64. Errors can be attributed to the film thickness and misalignment. Further refinement of the AR coat thickness will likely close the gap between the theoretical and measured gain.

5. Conclusion

An antenna on the flat surface of an immersion lens receives radiation more efficiently when illuminated through the substrate. The antenna response increases dramatically when the permittivity of the immersion lens is large and the curved surface is AR

coated. For the large signal gain to be maintained for all illumination angles, the AR coat must be uniform over the curved surface. As an alternative to LPCVD, a simple evaporation for depositing a uniform film on the hemispherical lens was presented. In this process, the curved surface is tilted relative to the source, which can be either electron-beam or thermal, and rotated throughout the deposition. Rotation at an angle of 70° generates a film with less than 10% thickness variation over a 120° full angle of the immersion lens. A theoretical model was developed and compared to profilometer measurements. In all cases, general agreement between measurement and theory has been demonstrated. A single dipole was fabricated onto the flat surface of an AR-coated germanium immersion lens. Substrate-side illumination generates an antenna response 49 ± 2.7 times greater than air-side illumination.

References

[1] C.R. Brewitt-Taylor, D.J. Guntun, H.D. Rees, Planar antennas on a dielectric surface, Electronics Letters 17 (20) (1981) 729–731.

[2] D.B. Rutledge, D.P. Neikirk, D.P. Kasilingam, Integrated-circuit antennas, Infrared and Millimeter Waves 10 (1983) 1–90.

[3] B. Lail, C. Middlebrook, P. Krenz, G.D. Boreman, Infrared dipole-coupled bolometer response on a hemispherical silicon immersion lens, Infrared Physics and Technology 52 (2009) 89–96.

[4] C. Middlebrook, P. Krenz, B. Lail, G.D. Boreman, Infrared phased-array antenna, Microwave and Optical Technology Letters 50 (4) (2008) 719–723.

[5] L. Martinu, O. Zabeida, A. Amassian, S. Larouche, C. Lavigne, J.E.K. Sapieha, D.E. Morton, F. Zimone, Plasma deposition of anti-reflective coatings on spherical lenses, Optical Interference Coatings WA7 (2001).

[6] H.M. Presby, C.A. Edwards, Near 100% efficient fibre microlenses, Electronics Letters 28 (1992) 582–584.

[7] D.Z. Rogers, Ball lenses for coupling and collimation, Lightwave 16 (1999) 104–110.

[8] M.A. George, D.Z. Rogers, LPCVD of optical interference coatings for micro-optical applications, Society of Vacuum Coaters (2000) 193–196.

[9] E.Y.M. Lee, N.H. Tran, R.N. Lamb, Growth of ZnS films by chemical vapor deposition of $Zn[S_2\ CN(CH_3)_2]_2$ precursor, Applied Surface Science 241 (2005) 493–496.

[10] C.T. Middlebrook, G. Zummo, G.D. Boreman, Direct-write electron-beam lithography of an IR antenna-coupled microbolometer onto the surface of a hemispherical lens, Journal of Vacuum Science and Technology B 24 (6) (2006) 2566–2569.

[11] M. Ohring, The Materials Science of Thin Films, Academic Press, 1992.